far as all predict the respective reactions to be non-synchronous and concerted.

Concluding Remarks

We have reported a comprehensive theoretical study of the cycloaddition reactions of ketene leading to the products diketene and 1,3-cyclobutanedione. Our results indicate that diketene should be the major product of the reaction of two ketenes, in agreement with experiment. Our predictions as to the energetics of these reactions are also in reasonable agreement with experiment.

Acknowledgment. This research was supported by the U.S. National Science Foundation, Grant No. CHE-8718469. All computations were carried out with the PSI suite of programs distributed by PSITECH, Inc., Watkinsville, Georgia.

Registry No. 1, 674-82-8; 2, 15506-53-3; ketene, 463-51-4.

Ab Initio Calculation of Secondary Deuterium Isotope Ratios in the Formation of Diketene

L. J. Schaad,* I. Gutman,† B. A. Hess, Jr.,* and Jiani Hu

Contribution from the Department of Chemistry, Vanderbilt University, Nashville, Tennessee 37235. *Received October 11, 1990*

Abstract: Ab initio calculations of deuterium isotope ratios in the formation of diketene agree with natural deuterium abundances reported for this molecule.

In 1986, Pascal, Baum, Wagner, Rodgers, and Huang[1] published a careful NMR study in which they were able to measure differences in naturally occuring deuterium concentrations in various positions of the compounds studied. In particular for diketene **1**, the ratio of deuterium on the exo methylene to that in the ring was 0.975 ± 0.026, and the concentration in the one exo position relative to the other was 1.040 ± 0.025.

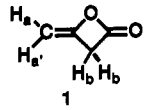

1

We report here ab initio calculations of deuterium isotope ratios in the formation of diketene from ketene. Calculated isotope ratios resulting from both secondary kinetic and equilibrium control are reported over the temperature range 100-600 K. Results are consistent with Pascal's observations.

Computations

Energy calculations, geometry optimizations, and vibrational frequency calculations were done by using the Cambridge University CADPAC program[2] on an SCS 40 computer. The built-in STO-3G, 3-21G, and 6-31G* basis sets were used in RHF calculations on ketene, diketene, the transition structure for the formation of diketene, and the diketene isomers cyclobutane-1,2-dione and cyclobutane-1,3-dione.

Moments of inertia and vibrational frequencies from CADPAC were used to calculate partition functions in the rigid-rotor-harmonic-oscillator approximation. These in turn gave rate and equilibrium constants for the required isotopomers.

Structures

Optimized RHF/6-31G* structures are shown in Figures 1 and 2 with energies in the STO-3G, 3-21G, and 6-31G* bases given in Table I. These structures agree with those of Seidl and Schaefer,[3,4] who give leading references into the literature of diketene and who discuss the interesting problem of why ketene dimerizes to diketene rather than to cyclobutane-1,3-dione. Harmonic vibrational frequencies were computed for all optimized species, and as expected all were real except for a single imaginary frequency of the transition structure.

† Permanent Address: Faculty of Science, University of Kragujevac, P.O. Box 60, 34000 Kragujevac, Yugoslavia.

Table I. Energies (au) of Optimized Structures

	STO-3G	3-21G	6-31G*
ketene	-149.726 105	-150.876 526	-151.724 672
diketene	-299.575 309	-301.779 262	-303.487 380
diketene transition structure	-299.381 164	-301.690 107	-303.394 561
cyclobutane-1,2-dione	-299.579 483	-301.777 479	-303.482 226
cyclobutane-1,3-dione	-299.579 960	-301.782 977	-303.489 561

Table II. Optimized RHF/6-31G* Geometry of the Transition Structure for the Formation of Diketene from Ketene

bond lengths (Å)		bond angles (deg)		dihedral angles (deg)[a]	
O_1C_2	1.223	$O_1C_2C_3$	140.8	$O_1C_2C_3H_4$	-3.5
C_2C_3	1.338	$O_1C_2C_8$	107.5	$O_1C_2C_3H_5$	178.6
C_2C_8	1.711	$C_2C_3H_4$	118.7	$O_1C_2C_8C_6$	-48.2
C_3H_4	1.073	$C_2C_3H_5$	122.3	$O_7C_6C_8C_2$	-52.2
C_3H_5	1.073	$C_2C_8C_6$	99.0	$O_7C_6C_8H_9$	74.5
C_6O_7	1.107	$C_6C_8H_9$	109.9	$O_7C_6C_8H_{10}$	-160.7
C_6C_8	1.413	$C_6C_8H_{10}$	109.0	$C_8C_2C_3H_4$	177.0
C_8H_9	1.081	$O_7C_6C_8$	175.6		
C_8H_{10}	1.081				

[a] The dihedral angle conventions of the CADPAC program are used. See Figure 2a,c for numbering.

Two ORTEP views of the transition structure for ketene dimerization are shown in Figure 2b,c. This structure agrees well with Seidl and Schaefer's result.[4] The reaction is far from synchronous, with the C_2-C_8 bond formation being more advanced than the C_6-O_1. This is in spite of the fact that this CO bond is shorter (1.358 Å) than the CC bond (1.508 Å) in the product. It may not be useful to force too close an analogy between this [2 + 2] cycloaddition and the related reaction of ethylene plus ethylene, since the double bonds involved in the ketene have fewer substituents and therefore lack most of the stereochemical consequences of the ethylene prototype. Further, the three-center

(1) Pascal, R. A., Jr.; Baum, M. W.; Wagner, C. K.; Rodgers, L. R.; Huang, D.-S. *J. Am. Chem. Soc.* **1986**, *108*, 6477.
(2) Amos, R. D.; Rice, J. E. *CADPAC: The Cambridge Analytic Derivatives Package*, Issue 4.0, Cambridge, 1987.
(3) Seidl, E. T.; Schaefer, H. F. *J. Am. Chem. Soc.* **1990**, *112*, 1493.
(4) Seidl, E. T.; Schaefer, H. F. preceding paper in this issue.

0002-7863/91/1513-5200$02.50/0

Table III. Isotope Effects on the Rate of Formation of Diketene at 300 K Computed with the 6-31G* Basis

isotope	position in transition structure[a]	$k_{unsubstituted}/k_{isotopomer}$ uncorrected	with tunnel correction	with frequency scaling	with scaling + tunneling
D	4	0.888	0.889	0.908	0.909
D	5	0.866	0.867	0.889	0.890
D	9	0.802	0.803	0.834	0.834
D	10	0.795	0.795	0.828	0.828
^{13}C	2	1.032	1.035	1.031	1.032
^{13}C	3	0.998	0.998	0.998	0.998
^{13}C	6	1.015	1.017	1.014	1.016
^{13}C	8	1.024	1.026	1.023	1.025
^{14}C	2	1.062	1.067	1.059	1.062
^{14}C	3	0.996	0.996	0.997	0.997
^{14}C	6	1.029	1.032	1.027	1.030
^{14}C	8	1.046	1.050	1.044	1.047
^{17}O	1	1.014	1.015	1.013	1.014
^{17}O	7	0.994	0.994	0.994	0.994
^{18}O	1	1.026	1.028	1.025	1.026
^{18}O	7	0.989	0.989	0.990	0.990

[a] This is the position as given by the numbering of Figure 2b,c. It also fixes the isotope position in the reactant ketene.

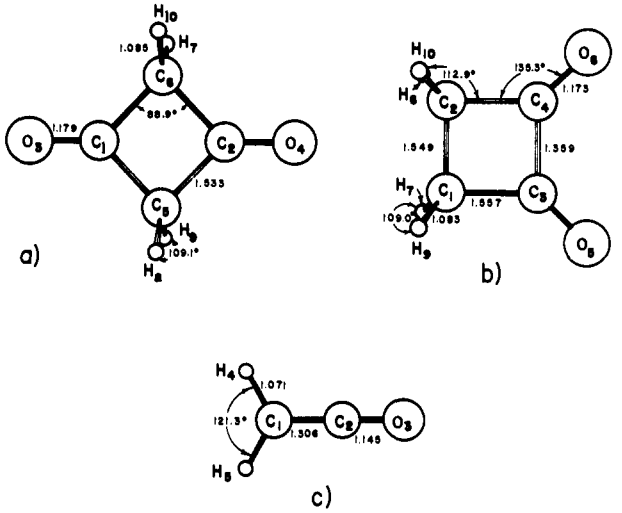

Figure 1. Optimized RHF/6-31G* structures. Distances are in angstroms, angles in degrees: (a) cyclobutane-1,3-dione, D_{2h}, (b) cyclobutane-1,2-dione, C_{2v}, (c) ketene, C_{2v}.

π system plus the extra perpendicular two-center π system on CO is quite different from the simple two-center π system of ethylene. Nevertheless, a comparison of Figure 2c with Figure 3, adapted from Woodward and Hoffmann's chapter on cycloadditions,[5] does incline us to describe the diketene formation as a $[2_s + 2_a]$ reaction. The key feature is that the ketene in the foreground of Figure 2c (containing $O_1C_2C_3$) is adding suprafacially to the ketene (containing $O_7C_6C_8$) in the back, while the back ketene is adding antarafacially to the front. In addition, $C_8H_9H_{10}$ and $C_2C_3H_4H_5$ lie in roughly perpendicular planes in a way that is consistent with the $[2_s + 2_a]$ addition in Figure 3 but not with the $[2_a + 2_a]$ nor with the $[2_s + 2_s]$ addition.

In the 6-31G* basis, diketene is computed to be more stable than two ketene monomers by 24 kcal/mol, and the transition structure is 34 kcal/mol above the two monomers. The 1,3-dione is 1.4 kcal/mol below diketene, while the 1,2 isomer is 3.2 kcal/mol above.

Isotope Ratios

Pascal[1] used a commercial sample of diketene whose synthesis is uncertain,[6] but it is probable that it was made by the dimerization of ketene.[7] In the usual preparation,[8] acetone is pyrolyzed

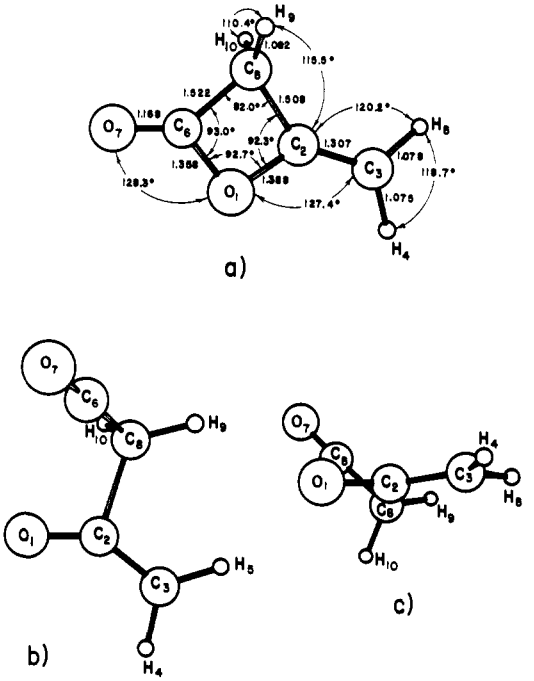

Figure 2. Optimized RHF/6-31G* structures. Distances are in angstroms, angles in degrees: (a) diketene, C_s, (b) and (c) transition structure for formation of diketene, C_1. Parameters of transition structure are given in Table II.

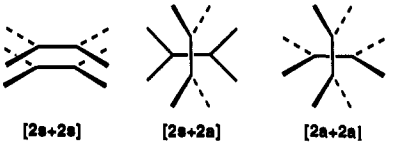

Figure 3. Idealized geometry in [2 + 2] cycloadditions (adapted from ref 5).

and the resulting ketene gas is collected at dry ice/acetone temperature (−77 °C). Since ketene can be reformed from diketene by heating[9] to 550 °C, all we can really say is that diketene is formed over some temperature range between −77 and +550 °C. Nor is it known whether the observed distribution is determined by rate or equilibrium or a mixture of both.

Since the natural deuterium abundance[1] is only about 0.015%, molecules with more than one deuterium atom are rare enough to be ignored in the following analysis. Let A be a ketene molecule

(5) Woodward, R. B.; Hoffmann, R. *The Conservation of Orbital Symmetry*; Verlag Chemie: Weinheim, 1970; Chapter 6.
(6) Technical Services, Aldrich Chemical Co., Inc., personal communication.
(7) Clemens, R. J. *Chem. Rev.* **1986**, *86*, 241.
(8) Horning, E. C., Ed. *Organic Synthesis*; Wiley: New York, 1955; Collect. Vol. III, p 508.
(9) Baumgarten, H. E., Ed. *Organic Synthesis*; Wiley: New York, 1973; Collect. Vol. V, p 679.

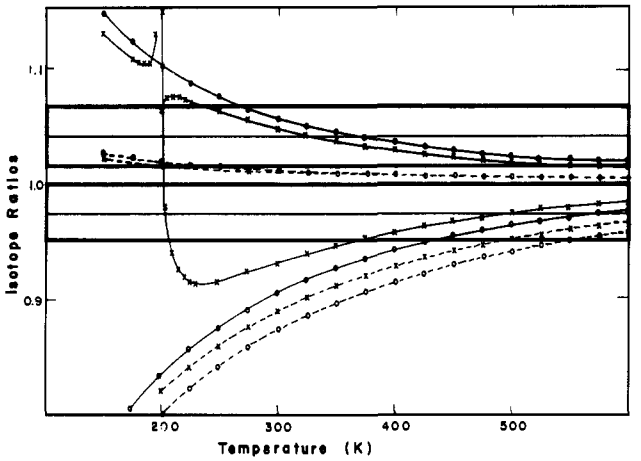

Figure 4. Isotope ratios in diketene formation computed with the STO-3G basis. The horizontal lines at isotope ratios of 1.040 and 0.975 are Pascal's observed ratios a′/a and (a + a′)/b, respectively. Heavy boxes show his estimated uncertainty. Solid lines give kinetic and dashed lines equilibrium isotopic ratios. Circles are uncorrected isotope ratios. Crosses show isotopic ratios corrected for tunneling and by scaling computed frequencies (kinetic ratios) or by scaling only (equilibrium ratios).

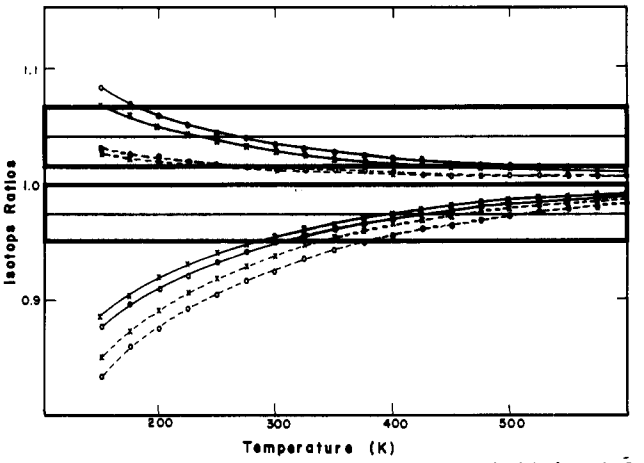

Figure 5. Isotope ratios in diketene formation computed with the 3-21G basis. Symbols have same meaning as in Figure 4.

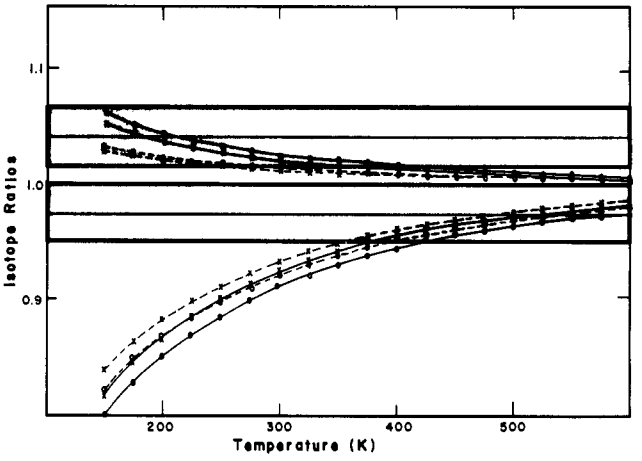

Figure 6. Isotope ratios in diketene formation computed with the 6-31G* basis. Symbols have same meaning as in Figure 4.

without deuterium and P_0 be the product diketene with no deuterium. Similarly, let B be ketene with a single deuterium and P_4, P_5, P_9, and P_{10} be, respectively, product with a single deuterium replacing H_4, H_5, H_9, or H_{10} of the transition structure numbered as in Figure 2b. Atoms H_4 and H_5 become the distinct exo methylene hydrogen atoms of the product (the H_a and $H_{a'}$ of Pascal[1]). Atoms H_9 and H_{10} are distinct in the transtion structure but become the equivalent ring hydrogens of the product (Pascal's H_b) so that products P_9 and P_{10} are indistinguishable. Assuming the formation of diketene is second-order in ketene and that product ratios are kinetically determined, the rate equations for the formation of these products are

$$d[P_0]/dt = k_0[A]^2 \quad (1)$$

$$d[P_4]/dt = k_4[A][B] \quad (2)$$

$$d[P_5]/dt = k_5[A][B] \quad (3)$$

$$d([P_9] + [P_{10}])/dt = k_9[A][B] + k_{10}[A][B] \quad (4)$$

The addition of eqs 2 and 3 followed by division by eq 4 gives after integration

$$\frac{[P_4(t)] + [P_5(t)]}{[P_9(t)] + [P_{10}(t)]} = \frac{k_4 + k_5}{k_9 + k_{10}} \quad (5)$$

The product ratio is independent of the reaction time and is just Pascal's ratio (a + a′)/b. Similarly Pascal's ratio a′/a is given by

$$[P_5(t)]/[P_4(t)] = k_5/k_4 \quad (6)$$

Analogously, if the product concentrations are determined by the equilibria

$$2A \overset{K_0}{\rightleftharpoons} P_0 \quad (7)$$

$$A + B \overset{K_4}{\rightleftharpoons} P_4 \quad (8)$$

$$A + B \overset{K_5}{\rightleftharpoons} P_5 \quad (9)$$

$$A + B \overset{K_9}{\rightleftharpoons} P_9 \quad (10)$$

then

$$\frac{a + a'}{b} = \frac{K_4 + K_5}{K_9} \qquad \frac{a'}{a} = \frac{K_5}{K_4} \quad (11)$$

These rate and equilibrium constants were computed as described above, and results obtained by the RHF method using STO-3G, 3-21G, and 6-31G* bases are shown in, respectively, Figures 4–6 over the temperature range 150–600 K. Frequencies computed by ab initio RHF methods are usually too high, so a rough correction was made by scaling all frequencies by a factor of $0.8^{1/2}$. Tunneling corrections were made by using Bell's eq 3.23 of ref 10, which uses a truncated inverted parabola as a model for the potential surface. This correction is only the first term of a more complete expression, and it can become infinite for certain combinations of temperature and frequency. It is this and not a failure of the STO-3G basis that causes the peculiar behavior of the corrected kinetic curves near 200 K in Figure 4. This fault could be cured by using Bell's full expression, but Bell[10] recommends simply interpolating past the troublesome point. For simplicity, results of scaling or tunneling corrections alone on the kinetic effect are not shown in Figures 4–6. They are not dramatically different from the curves given.

All the curves in Figures 4–6 (ignoring the singularity near 200 K in the STO-3G results) do agree with Pascal's measurements in the rough sense that the a′/a ratio is larger than (a + a′)/b. A closer look shows the assumption of kinetic control of these ratios to be better than that of equilibrium control. There is no temperature range with any of the three bases over which both ratios are simultaneously computed to lie in the observed regions for the equilibrium curves. The 3-21G results for kinetic control give the best fit to experiment, with both ratios computed to be in the experimental range from about 35 to 210 °C for the uncorrected and from 15 to 150 °C for the corrected data. The STO-3G results show somewhat poorer and the 6-31G* results considerably

(10) Bell, R. P. *The Tunnel Effect in Chemistry*; Chapman and Hall: London, 1980.

poorer agreement with experiment. However, not too much should be made of this given the uncertain conditions of commercial diketene formation. About all that should be said is that, in a rough way, calculations of the kinetic isotope effects are in accord with Pascal's observed deuterium ratios. The experimental measurement of these isotope effects at a known temperature would be worthwhile.

A minor point concerns Pascal's comment that $(a + a')/b = 0.975$ suggests an inverse secondary kinetic isotope effect for the dimerization of ketene. Although Table III shows that kinetic isotope effects on the rate of diketene formation are computed to be inverse for all positions of deuterium substitution, this conclusion does not seem to follow from Pascal's results. Table III also lists several kinetic isotope effects of oxygen and carbon isotopomers.

Finally, a point of Pascal's that is strongly supported by our calculations is his tentative assignment of H_a in diketene as the hydrogen cis to the ring oxygen and $H_{a'}$ as cis to the ring carbon. With this assumption, all our calculations give $a'/a > 1$, as found by experiment.

Acknowledgment. We thank the Fulbright Program for a Fellowship to I.G. during the tenure of which this work was carried out. We are also grateful to the National Science Foundation for a grant (CHE 8808018) that allowed the purchase of our SCS 40 computer.

Effect of Electron Correlation on the Electrostatic Potential Distribution of Molecules

F. J. Luque,*,† M. Orozco,‡ F. Illas,§ and J. Rubio§

Contribution from the Departament de Farmacia, Unitat Fisicoquimica, Facultat de Farmàcia, Universitat de Barcelona, Avgda. Diagonal s/n, 08028 Barcelona, Spain, and Departament de Bioquimica i Fisiologia and Departament de Quimica Fisica, Facultat de Quimica, Universitat de Barcelona, C/. Martí i Franques 1, 08028 Barcelona, Spain. *Received September 19, 1990*

Abstract: A study on the effect of the electron correlation on the electrostatic potential distribution in molecules is presented. The study is focused not only on the features of the molecular electrostatic potential (MEP), but also on the atomic charges and dipoles. Electron correlation is introduced by means of the CIPSI and full-CI methods by using both 6-31G* and 6-31G basis sets. The results reported in this paper clearly point out the reliability of the CIPSI method to reproduce the features of the MEP evaluated from full-CI wave functions. Comparison of MEPs computed from SCF and full-CI wave functions indicates that the electron correlation does not have a uniform effect on the MEP in the whole space surrounding the molecule. Thus, electron correlation has a relevant effect near the nuclei, but the MEP determined from the SCF wave function remains largely unaffected in regions located outside the van der Waals sphere. Indeed, the characteristics of the SCF MEP minima undergo only a small change when electron correlation is considered.

Introduction

The inclusion of electron correlation in quantum chemical studies is becoming a usual practice due to the need for precisely determining both the total energy and the molecular properties. One of these properties is electron density, which is highly informative about the reactivity characteristics of molecules. Since the early quantum chemical studies, a large amount of research effort has been focused on the description of the electron density distribution and other related molecular properties within the Hartree-Fock framework. Nevertheless, less attention has been devoted to determine the influence of the electron correlation on the electron density,[1] even though this effect is expected to be essential in order to obtain a reliable picture of the electron density distribution and of related molecular properties.[2]

After the early work of Daudel et al.,[2b] several studies on the electron correlation modulation of properties related to the molecular electrostatic distribution have been reported. Amos et al.[3] investigated the changes in the molecular multipole moments computed from configuration interaction and perturbation theory with regard to those evaluated at the SCF level. Hehre et al.[4] and Cioslowski[5] recently examined the effect of the electron correlation on atomic charges by means of calculations at both SCF and second-order Moller-Plesset levels. However, to our knowledge, systematic studies on the effect of the electron correlation on the electrostatic distribution have not previously been reported.

The relevance of the molecular electrostatic potential (MEP) in determining chemical reactivity has been stressed elsewhere.[6-11]

† Departament de Farmàcia.
‡ Departament de Bioquimica i Fisiologia.
§ Departament de Quimica Fisica.

(1) (a) Wang, L. C.; Boyd, R. J. *J. Chem. Phys.* **1989**, *90*, 1083. (b) Boyd, R. J.; Wang, L. C. *J. Comput. Chem.* **1989**, *10*, 367. (c) Gatti, C.; MacDougall, D. J.; Bader, R. F. W. *J. Chem. Phys.* **1988**, *88*, 3792 and references therein.

(2) Szabó, A.; Ostlund, N. S. *Modern Quantum Chemistry*; MacMillan: New York, 1982. (b) Daudel, R.; LeRouzo, H.; Cimiraglia, R.; Tomasi, J. *Int. J. Quantum Chem.* **1978**, *13*, 537.

(3) (a) Amos, R. D. *Chem. Phys. Lett.* **1980**, *73*, 602. (b) Amos, R. D. *Chem. Phys. Lett.* **1985**, *113*, 19.

(4) Carpenter, J. E.; McGrath, M. P.; Hehre, W. J. *J. Am. Chem. Soc.* **1989**, *111*, 6154.

(5) Cioslowski, J. *J. Am. Chem. Soc.* **1989**, *111*, 8333.

(6) Scrocco, E.; Tomasi, J. *Top. Curr. Chem.* **1973**, *42*, 95.

(7) (a) Politzer, P.; Daiker, K. C. In *The Force Constant in Chemistry*; Deb, B. M., Ed.; Van Nostrand Reinhold: New York, 1981; p 294. (b) *Chemical Applications of Atomic and Molecular Electrostatic Potentials*; Politzer, P., Truhlar, D. G., Eds.; Plenum Press: New York, 1981. (c) Náray-Szabó, G.; Surján, P. R. In *Theoretical Chemistry of Biological Systems*; Náray-Szabó, G., Ed.; Elsevier: Amsterdam, 1986; p 1.

(8) (a) Kollman, P.; McKelvey, J.; Johansson, A.; Rothenberg, S. *J. Am. Chem. Soc.* **1975**, *97*, 955. (b) Kollman, P.; Rothenberg, S. *J. Am. Chem. Soc.* **1977**, *99*, 1333. (c) Kollman, P. *J. Am. Chem. Soc.* **1977**, *99*, 4875. (d) Scrocco, E.; Tomasi, J. *Adv. Quantum Chem.* **1978**, *11*, 115. (e) Náray-Szabó, G. *Acta Phys. Acad. Sci. Hung.* **1981**, *51*, 65. (f) Politzer, P.; Landry, S. J.; Warnheim, T. *J. Phys. Chem.* **1982**, *86*, 4767. (g) Politzer, P.; Abrahmsen, L.; Sjoberg, P. *J. Am. Chem. Soc.* **1984**, *106*, 855.

0002-7863/91/1513-5203$02.50/0